A Hierarchical Horizon Detection Algorithm

Yu-Fei Shen, Dean Krusienski, Jiang Li, and Zia-ur Rahman

***Abstract*—A hierarchical elastic computer-aided detection algorithm is proposed to automatically detect the horizon in an aerial image. A hierarchical strategy, including coarse-level detection and fine-level adjustment, is applied. First, the original image is blurred by a large-scale low-pass filter. Then, a Canny edge detector and Hough transform are successively utilized to find major edges in the image and identify lines associated with those major edges. The desired horizon is modeled by the resulting line that best satisfies certain criteria. By doing so, the general position of the horizon can be quickly detected at the coarse-level step. Since the horizon is often not a straight line, an elastic fine-level adjustment is applied to capture the precise curvature of the horizon. A quantitative performance metric is designed, and preliminary experimental results show the feasibility and reliability of the proposed algorithm.**

***Index Terms*—Horizon detection.**

I. Introduction

HORIZON detection often serves as a preliminary step of many aerial or ground-based robotic systems [1]–[3]. A reliable segmentation of the sky and the ground plays an important role to subsequent steps. Much previous work has been conducted in horizon detection. Williams and Howard proposed a horizon detection algorithm for a specific ground-based rover application to segment the foreground plane from distant mountains and the sky in glacial environments [4]. Due to the specialty of that application, two strong but reasonable assumptions are made: 1) It is assumed that the bottom one-third of the image is ground, because the camera is mounted on a ground-based rover, and 2) the ground is assumed to appear all white with very little variance, because the rover is in glacial environments. Based on those two assumptions, the edge map, generated by applying a Canny edge detector [5] to the original image, is examined column by column. An edge point in a column can be considered a point of the horizon when pixels below it in that column appear all white with little variance. The problem of that algorithm is that the two assumptions often fail in other environments; thus, it will not be further considered for the present approach. Dusha *et al.* [6] applied the Hough transform [7] to recognize straight lines from the binary edge map, which is also generated by using a Canny edge detector [5], based on the assumption that the horizon is the strongest boundary in the image. However, that assumption is not always valid, and that method can be easily disturbed by the appearance of other strong edges. Ettinger *et al.* proposed a horizon detection method in a greedy search manner [3], based on two assumptions: 1) The horizon is a straight line that partitions the image into two regions, namely, sky and ground, and 2) there is little variance in either region, i.e., the pixel characteristics of the sky region are consistent and different from those of the ground region and vice versa. Thus, the detection of the horizon becomes to search for the optimal straight line such that the sum of the variances of both regions reaches the lowest value. Lines of all possible locations and angles are tested, and the optimal one that meets the aforementioned criterion is considered the horizon. Two problems of that method are found: 1) It is computationally expensive due to the greedy search scheme, and 2) the second assumption fails when large objects having similar color to the sky appear in the ground region of the image, such as lakes, rivers, or other large bodies of water.

In this letter, we propose an automatic horizon detection algorithm with a hierarchical strategy in which the nonhorizon pixels are gradually excluded step by step. The proposed algorithm is designed with several relatively soft decisions, in which a refined detection mechanism is utilized, in order to adapt to practical horizon imaging scenarios. Specifically, it consists of a coarse-level detection and a fine-level adjustment. First, the original image is blurred by a large-scale low-pass filter. Then, a Canny edge detector [5] and Hough transform [7] are successively utilized to find major edges in the image and identify lines associated with those major edges. The desired horizon is modeled by one of the lines. Since the horizon is often not a straight line, an elastic fine-level adjustment is applied to capture the curvature of the horizon.

The remainder of this letter is organized as follows. In Section II, we describe the proposed horizon detection algorithm in detail. The experimental results are shown in Section III, followed by the conclusions in Section IV.

II. Methods

The proposed hierarchical horizon detection algorithm consists of a coarse-level detection and a fine-level adjustment. The following three steps comprise the coarse-level detection. Three steps, namely, (1) major edge detection, (2) line fitting, and (3) coarse adjustment, comprise the coarse level detection. (1) The original image as shown in Fig. 1 is blurred by a large-scale low-pass filter to remove relatively fine edges and retain relatively major edges in the image. In this letter, we employ a Gaussian low-pass filter with a relatively large sigma σ which is adaptive to the dimension of the image, i.e., $\sigma = N_V/50$,

Manuscript received November 7, 2011; revised February 14, 2012 and March 27, 2012; accepted April 3, 2012. Date of publication May 15, 2012; date of current version September 7, 2012. This work was supported by the National Aeronautics and Space Administration (NASA) Aviation Safety Program under NASA Cooperative Agreement NNL07AA02A with Old Dominion University.

Y.-F. Shen, D. Krusienski, and J. Li are with the Department of Electrical and Computer Engineering, Old Dominion University, Norfolk, VA 23529 USA (e-mail: yshen002@odu.edu; dkrusien@odu.edu; jli@odu.edu).

Z. Rahman, deceased, was with the Electromagnetics and Sensors Branch, Langley Research Center, National Aeronautics and Space Administration, Hampton, VA 23681 USA.

Color versions of one or more of the figures in this paper are available online at http://ieeexplore.ieee.org.

Digital Object Identifier 10.1109/LGRS.2012.2194473

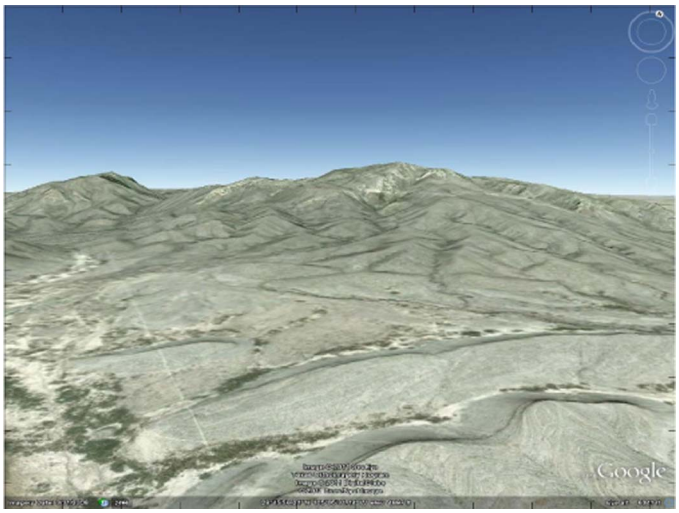

Fig. 1. Sample image.

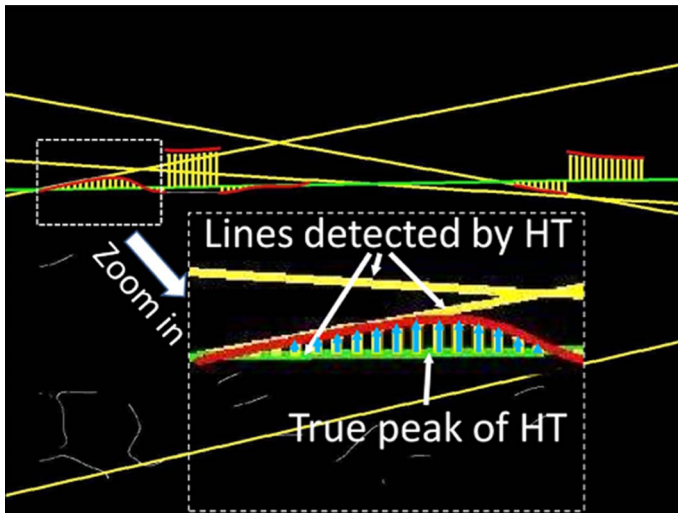

Fig. 2. Coarse adjustment.

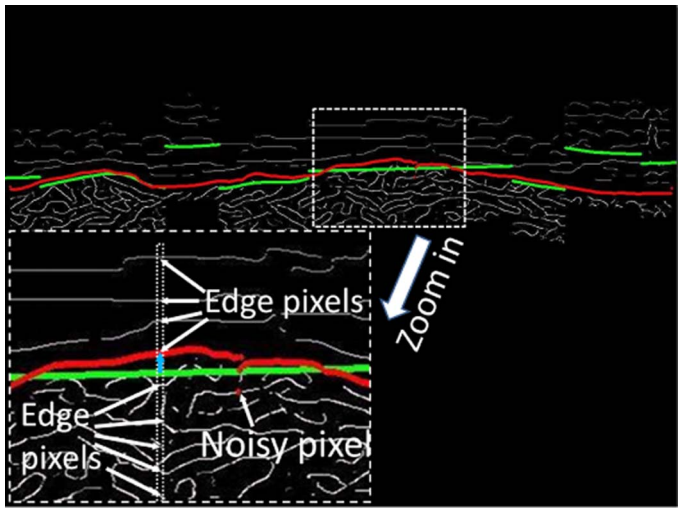

Fig. 3. Fine adjustment.

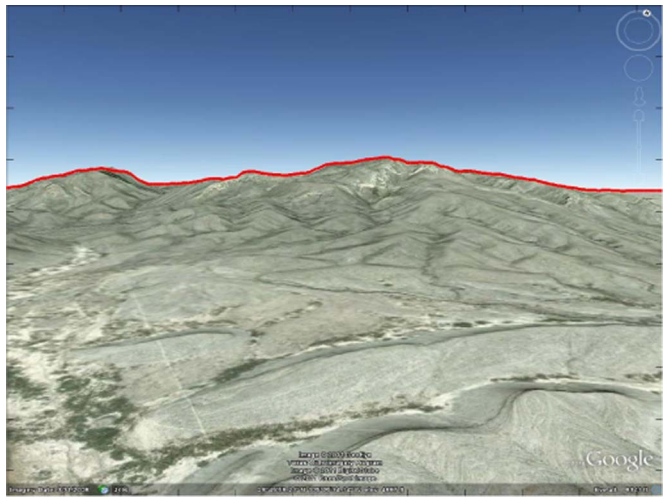

Fig. 4. Detected horizon.

where N_V is the number of rows in the image. Then, a Canny edge detector [5] is applied to the blurred image to find major edges. The reason that we make use of the Canny edge detector is because it provides edge strength information in addition to edge location information. (2) An edge strength histogram is computed based on the edge strength produced by the Canny edge detector, and the top $p\%$ of the points are obtained as possible points that comprise the horizon. On the one hand, p should be a small number because the horizon is often the strongest edge in the image. On the other hand, it is not always the case, so p should not be too small. In other words, we would rather conservatively include some nonhorizon points in this step and exclude them in a later step than frivolously lose some of the key horizon points in this step. Empirically, $p\%$ is adaptively obtained as $5/N_H$, where N_H is the number of columns in the image. A binary edge map consists of the top $p\%$ strongest edge points that can be generated. The standard Hough transform (SHT) [7] is then applied to fit probable lines in the binary edge map. Due to the presence of strong edges in addition to the horizon in the image, the highest peak of the voting result of the SHT does not necessarily correspond to the horizon. Thus, it is unreliable to simply take the highest peak as the horizon. Instead, the top N_L highest peaks are taken into account by comparing the average edge strengths within the dual-side narrow bands along each of them. The line that has the highest average edge strength within its dual-side narrow bands is called the true peak of Hough transformation. Empirically, N_L is set to five. This soft decision strategy makes the detection more reliable and robust. In Fig. 2, the green line is the true peak of Hough transformation, along with four yellow lines which are among the top N_L highest peaks but not the true peak. (3) It is necessary to adjust the coarsely detected line, because the real horizon is often not perfectly straight. The coarse-level adjustment is to search the dual-side neighborhood of each pixel of the detected line according to the edge map of the blurred image. As shown in Fig. 2, the yellow arrows denote the directions of the coarse adjustment, and the red dots denote the position of each point after the coarse adjustment.

A fine adjustment takes place after the position of the horizon is coarsely determined. As shown in Fig. 3, the neighborhood of the coarsely detected horizon is explored based on a fine edge map computed from the original image in which fine edges are retained. The coarsely detected horizon pixels are then adjusted again to positions that meet certain criteria. The criterion used in [8] is to check edge pixels within the dual-side bands and find the one with the largest

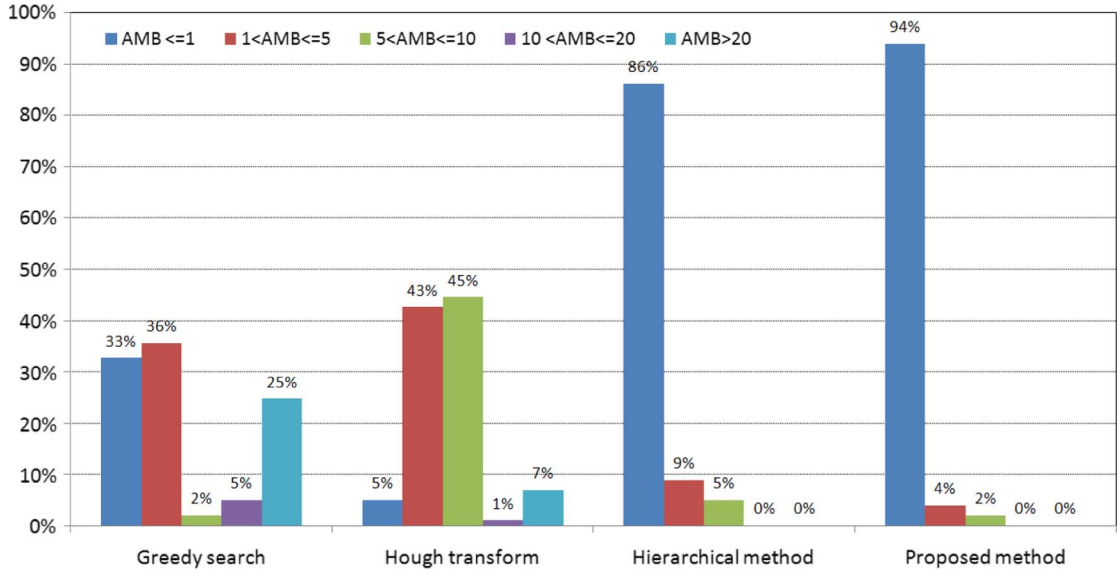

Fig. 5. Horizon detection results by using the greedy search method [3], the Hough transform [6], the hierarchical method [8], and the proposed method.

edge strength. In general, it works well. However, strong edge patterns occasionally appear very close to the horizon, and the pixel of the horizon may not be the strongest edge point in its neighborhood. Therefore, in this letter, we check a set of the strongest pixels EP, which is defined as

$$EP = \{E_i | ES_i \geq ES_{\max} \times 0.8,\ i = 1, 2, \ldots, N_E\} \quad (1)$$

where N_E is the total number of edge pixels in that 60-pixel-wide neighborhood, ES_i $(i = 1, 2, \ldots, N_E)$ is the edge strength of the ith strongest edge pixel E_i, and $ES_{\max}$ is the edge strength of E_1. Let N_{TE} be the number of points in EP and TE_j $(j = 1, 2, \ldots, N_{TE})$ be the jth strongest edge point in EP. We employ a modification of the idea in [3] by computing the variance of TE_j's dual-side neighborhood. When validated on a test image database, in most cases, the true horizon pixel is the edge pixel that has the lowest variances of its dual-side neighborhood. This is formulated as $v_j = \sqrt{\text{var}(NB_j^+) \times \text{var}(NB_j^-)}$, where NB_j^+ and NB_j^- are the upper and lower neighborhoods of TE_j, respectively, and v_j is the variance measurement to be evaluated. TE_H is considered the pixel of the horizon when its corresponding v_H is the minimum value of v_j. Noisy points may emerge due to the discontinuity of the horizon in the fine edge map. We remove these discontinuous points by interpolation based on their neighboring points on the left and right. In this letter, we use the B-spline interpolation method [9], [10]. After removing all the noisy points, a smoothing technique is applied to local segments of the detected horizon to get the smooth final detection result as shown in Fig. 4.

III. Experimental Results

The proposed algorithm is tested on 100 remote sensing images, which are in the JPG format with a resolution of 1144 × 948 pixels downloaded from Google Earth. The test images are captured in various view angles, over different types of terrains, and at different elevations that range from 1000 to 30 000 ft. On the same image set, the greedy search method [3], the Hough transform method [6], and the hierarchical method [8] are tested. The quantitative performance measurement, i.e., the average maximum bias (AMB) [8], is utilized. AMB is defined as

$$AMB = \frac{1}{H_M} \sum_{h=1}^{H_M} MB_h, \qquad H_M = L_H \times 0.1 \quad (2)$$

where L_H is the total pixel number of the detected horizon, H_M is one-tenth of L_H, and MB_h $(h = 1, 2, \ldots, H_M)$ is the hth maximum bias from the detected horizon to the position of the true horizon in the unit of pixels. Evaluating the average bias of the worst detected segment can reveal the true performance of the method, avoiding the significant bias canceled out by well-aligned segments. That is, if the most biased segment of the detection result can be considered satisfactory, the rest of the detected horizon can be guaranteed to be better than the most biased segment. Fig. 5 shows the horizon detection results by using the four methods. Five AMB intervals are used, which are, respectively, according to perfect detection $(AMB \leq 1)$, good detection $(1 < AMB \leq 5)$, acceptable detection $(5 < AMB \leq 10)$, biased detection $(10 < AMB \leq 20)$, and false detection $(AMB > 20)$. The percentage shown above the bar of each AMB interval reflects the ratio of the number of images, of which the AMB value falls into that AMB interval, to the total number of tested images. The greedy search method finds the true horizon in 69% of the test (33% perfect detection and 36% good detection), although it fails in 25% of the test when large bodies of water or anything that has similar color to the sky appears in the ground region of the image. These cases cannot achieve better detection because of the straight line assumption, although the general position of the horizon is detected. The Hough transform method, due to its intrinsic mechanism, is easily corrupted by other nonhorizon edges shown in the image. This explains why it only achieves 5% perfect detection but high rates of good and acceptable detection (43% and 45%, respectively). In particular, when the nonhorizon edges are stronger than the horizon, it fails as shown in the 7% of false detection. The proposed method achieves 94% perfect detection and 4% good detection, showing the improvement to the hierarchical method [8] which generates

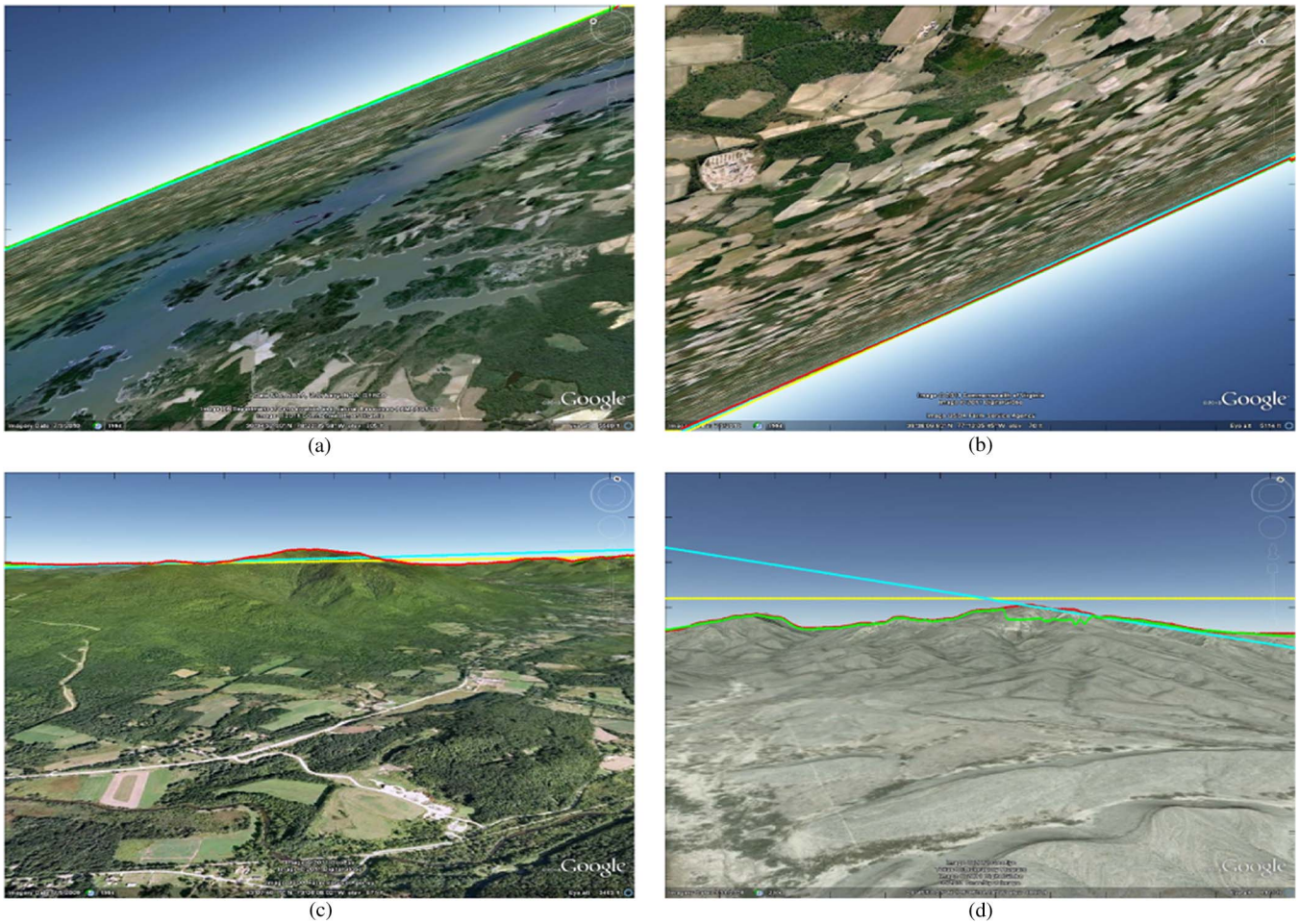

Fig. 6. Detection results by using (yellow) the greedy search method [3], (cyan) the Hough transform [6], (green) the hierarchical method [8], and (red) the proposed method.

86% perfect detection and 9% good detection. It is worth noting that the latter two methods produced no false detections on the test images. Fig. 6 shows a comparison of the detection results generated by the four methods, in yellow, cyan, green, and red, respectively. All four methods detect the horizon in Fig. 6(a) and (b). In Fig. 6(c), the former two methods find the general position of the horizon but cannot fit its curvature due to the straight line assumption. The latter two methods accurately find the horizon. In Fig. 6(d), the former two methods fail. The hierarchical method [8] finds the true horizon with minor bias. The proposed method successfully detects the horizon.

IV. Conclusion

By using a refined Hough transform to roughly detect the horizon and then precisely adjusting it in its dual-side neighborhood, the proposed algorithm greatly improves the detection accuracy compared to traditional methods. The promising results show the feasibility of the proposed algorithm. It provides a useful tool for horizon detection, which is often an inevitable preliminary step of vision-based robotic systems.

Acknowledgment

The authors deeply cherish the memory of Dr. Rahman and his outstanding leadership and contribution in this study.

References

[1] N. Pears and B. Liang, "Ground plane segmentation for mobile robot visual navigation," in *Proc. IEEE Int. Conf. Intell. Robots Syst.*, 2001, vol. 3, pp. 1513–1518.

[2] Y. Kim and H. Kim, "Layered ground floor detection for vision-based mobile robot navigation," in *Proc. IEEE ICRA*, 2004, vol. 1, pp. 13–18.

[3] S. Ettinger, M. Nechyba, P. Ifju, and M. Waszak, "Towards flight autonomy: Vision-based horizon detection for micro air vehicles," in *Proc. Florida Conf. Recent Adv. Robot.*, 2002.

[4] S. Williams and A. M. Howard, "Horizon line estimation in glacial environments using multiple visual cues," in *Proc. IEEE ICRA*, 2011, pp. 5887–5892.

[5] J. Canny, "A computational approach to edge detection," *IEEE Trans. Pattern Anal. Mach. Intell.*, vol. PAMI-8, no. 6, pp. 679–698, Nov. 1986.

[6] D. Dusha, W. Boles, and R. Walker, "Attitude estimation for a fixed-wing aircraft using horizon detection and optical flow," in *Proc. 9th Biennial Conf. Australian Pattern. Recognit. Soc. Digital Object Digit. Image Comput. Tech. Appl.*, 2007, pp. 485–492.

[7] R. O. Duda and P. E. Hart, "Use of the Hough transformation to detect lines and curves in pictures," *Commun. ACM*, vol. 15, no. 1, pp. 11–15, Jan. 1972.

[8] Y.-F. Shen, Z. Rahman, D. Krusienski, and J. Li, "A vision-based automatic safe landing-site detection system," *IEEE Trans. Aerosp. Electron. Syst.*, in press.

[9] D. Rueckert, L. I. Sonoda, C. Hayes, D. L. G. Hill, M. O. Leach, and D. J. Hawkes, "Nonrigid registration using free-form deformations: Application to breast MR images," *IEEE Trans. Med. Imag.*, vol. 18, no. 8, pp. 712–721, Aug. 1999.

[10] S. Lee, G. Wolberg, and S. Y. Shin, "Scattered data interpolation with multilevel B-splines," *IEEE Trans. Vis. Comput. Graph.*, vol. 3, no. 3, pp. 228–244, Jul.–Sep. 1997.